THE JOURNAL OF PHYSICAL CHEMISTRY B

Article

pubs.acs.org/JPCB

Investigation of the Photobleaching Process of Eosin Y in Aqueous Solution by Thermal Lens Spectroscopy

L. S. Herculano,* L. C. Malacarne, V. S. Zanuto, G. V. B. Lukasievicz, O. A. Capeloto, and N. G. C. Astrath*

Departamento de Física, Universidade Estadual de Maringá, Av. Colombo 5790, Maringá - PR, 87020-900, Brazil

ABSTRACT: Eosin Y is known to be a powerful probe of biological molecules and an efficient photosensitizing agent for the production of singlet molecular oxygen. Under continuous laser excitation, degradation through photobleaching is observed in aqueous solutions of eosin Y; this process is driven by the production of singlet oxygen. Optical bleaching in aqueous solutions is known to yield anomalous thermal lens transient signals, which can be evaluated by modeling the relaxation processes that give rise to the generation of heat in the solution. A model describing photobleaching in the thermal lens transient signal is derived and is applied to investigate eosin Y in aqueous solutions at different temperatures. Using this model, quantitative information regarding the molecular diffusion rate, optical bleaching, and fluorescence quantum efficiency is obtained.

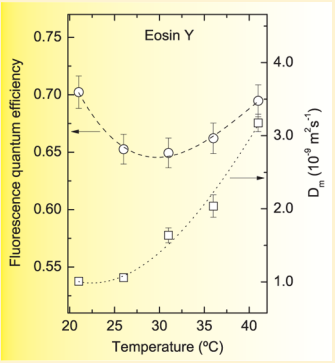

INTRODUCTION

Eosin Y is a halogenated derivative of the xanthene dye fluorescein. Its fluorescent properties are highly dependent on variations in its environment,[1−5] such as solvent polarity and the presence of cationic surfactants; the environment-dependent fluorescence makes this organic dye a powerful probe of biological molecules. The applications of eosin Y include detection of submicrogram quantities of a wide range of proteins,[6,7] use in dye-sensitized solar cells,[8−11] photodynamic inactivation of viruses and cells and phototherapy for cancer,[12−14] in which eosin Y is used as an efficient photosensitizing agent to produce singlet molecular oxygen[5,15−17]—ground state molecular oxygen.

Numerous studies have been published over the past few decades on singlet oxygen.[1,13,14,18,19] Of particular importance to singlet oxygen's photochemical and photobiological processes, the resistance of dyes toward photodegradation has been systematically studied.[18,19] Although the role of singlet oxygen in photochemical reaction kinetics is mostly inferred from the photoproducts, the mechanisms of reactions with singlet oxygen are often unknown[19] or not easily identified.

There are several methods for detecting the kinetics of the reactions of singlet oxygen in solutions and the photobleaching-based degradation effects of singlet oxygen on fluorescein molecules. One of these methods, emission spectroscopy, measures the emission of singlet oxygen at 1270 nm[20−22]—this wavelength has a very low emission quantum yield, which reduces the sensitivity of this method. Alternatively, indirect methods, such as flash photolysis and reactive solutions, have been used.[20] In addition, time-resolved thermal lens spectroscopy has been very successful in determining the absolute quantum yield for production of singlet molecular oxygen[23−25] as well as the quantum yields of fluorescence from different sensitizers.[26] This method has very high sensitivity and detects the kinetics of reactions in very dilute solutions.[27−29] Furthermore, thermal lens spectroscopy has been applied to investigate the optical bleaching and nonlinear absorption photophysics of organic dyes. These characteristics make this technique an attractive candidate for use in studying the effects of optical degradation on the thermal, optical, and molecular properties of eosin Y during photobleaching.

The thermal lens signal results from changes in the refractive index of the sample; these changes are generated by the heating produced from the optical absorption of a laser beam. The signal is proportional to the optical absorption coefficient of the sample; therefore, the signal is sensitive to changes in the concentration of the absorbing species. Recently, we applied this method to investigate photoinduced chemical reactions in aqueous solutions[30−33] and hydrocarbon fuels.[34] The theoretical description of the thermal lens effect employed in those studies relied on the time dependence of the optical absorption coefficient from changes in the concentration of the absorbing species within the excited volume of the sample. Here, we report a theoretical analysis and experimental measurements that consider signals from thermal, optical bleaching and mass diffusion effects during laser-induced local heating in aqueous solutions.

In this work, we investigate the temperature dependence of molecular diffusion and the kinetics of the reactions of aqueous solutions of eosin Y using time-resolved thermal lens spectroscopy. A theoretical model is used to describe the different contributions to the convoluted thermal lens signal,

Received: December 4, 2012
Revised: January 15, 2013
Published: January 17, 2013

   dx.doi.org/10.1021/jp3119296 | J. Phys. Chem. B 2013, 117, 1932−1937

and the time-dependent degradation of eosin Y through photobleaching is measured. Quantitative information regarding molecular diffusion and the reaction rate is obtained for temperatures ranging from 21 to 41 °C. Additionally, the fluorescence quantum efficiency is measured in the same temperature range.

THEORY

In the thermal lens experiments considered in this work, the continuous excitation and probe beams pass through the same volume of a liquid sample. The excitation is provided by a Gaussian-shaped laser beam, which produces a temperature gradient with approximately the same radial distribution. The refractive index changes according to the temperature distribution, creating a lens-like optical element in the sample. The effect is monitored by measuring the time-dependent intensity of the central portion of the Gaussian probe beam in the far-field region.

To model the contributions to the thermal lens signal, we consider optical bleaching in the illuminated volume as follows. The theory describing this effect has been presented recently.[30−34] Here, we elaborate on the approximations considered in these previous works. Assuming that the absorbed light energy can induce a chemical reaction in a photoreacting solution, the concentration of the absorbing species is modified in the excited volume, generating a mass (species) gradient. This phenomenon creates a time-dependent and spatially dependent absorption coefficient, which alters the signal accordingly. The time-dependent absorption coefficient can be written in terms of the species concentration $C(r, t)$ as $\beta(r, t) = C(r, t)\varepsilon$, where ε is the molar optical absorption coefficient. In a very dilute solution, the relaxation processes can be assumed to be first-order or pseudo-first-order, and the time dependence of the species concentration is given by the solution of the following differential equation

$$\frac{\partial}{\partial t}C(r, t) - D_m\nabla^2 C(r, t) = -\frac{2P_e}{\pi\omega_{0e}{}^2}\frac{\sigma}{h\nu}e^{-2r^2/\omega_{0e}{}^2}C(r, t) \tag{1}$$

where σ is the reaction cross section, h is Planck's constant, ν is the optical frequency, D_m is the mass diffusion coefficient, and ω_{0e} and P_e are the radius and the optical power of the excitation laser beam. The diffusion term in eq 1 accounts for the movement of photochemically modified species from outside to inside the excited volume by Brownian motion. It is assumed that the drift of particles because of the thermal gradient (Soret effect) and convection effects does not contribute to the concentration changes. The term on the right side of eq 1 accounts for the distorted Gaussian shape of the initial energy density of the excited state because of photobleaching.[28]

Although it is highly desirable to have a closed-form solution to eq 1, an analytical expression is only possible under approximations for the spatial distribution of the concentration. Under moderate excitation power, the solution for this equation can be determined by assuming a spatial average of each term of the concentration equation as $C(t) = \langle C(r, t)\rangle_r$. This, in turn, results in a simple form for the effective rate equation, $dC(t)/dt = -K_T C(t)$. Here, the total reaction rate K_T represents the averaged rates of photobleaching and movement because of molecular diffusion. The total absorption coefficient can be written in terms of the equilibrium ratio between the molar absorptivities of the products and reactants, $\bar{\varepsilon}$, in the illuminated volume by $\beta(t) = \beta[(1 - \bar{\varepsilon})e^{-K_T t} + \bar{\varepsilon}]$. β is the absorption coefficient at $t = 0$.

The time-dependent optical absorption coefficient acts directly on the temperature distribution in the sample and consequently acts directly on the signal. Assuming an isotropic and weakly absorbing material, the distribution of the temperature rise is described by the differential equation for heat conduction

$$\frac{\partial}{\partial t}T(r, t) - D_{th}\nabla^2 T(r, t) = Q_0\beta[(1 - \bar{\varepsilon})e^{-K_T t} + \bar{\varepsilon}]e^{-2r^2/\omega_{0e}{}^2} \tag{2}$$

where $D_{th} = k/(\rho c)$ is the thermal diffusivity, k is the thermal conductivity, ρ is the mass density, and c is the specific heat of the sample. β is the optical absorption coefficient of the reactants. $Q_0 = 2P_e\varphi/(\rho c\pi\omega_{0e}{}^2)$, where φ is the fraction of the absorbed energy available for conversion to heat. The sample is treated as an infinite medium with respect to the excitation beam. The heat conduction equation is solved using integral transform methods yielding[31]

$$T(r, t) = Q_0\beta\left[\bar{\varepsilon}\int_0^t \frac{e^{-(2r^2/\omega_{0e}{}^2)/(1+2\xi/t_c)}}{1 + 2\xi/t_c}\,d\xi + (1 - \bar{\varepsilon})e^{-K_T t}\int_0^t e^{-K_T\xi}\frac{e^{-(2r^2/\omega_{0e}{}^2)/(1+2\xi/t_c)}}{1 + 2\xi/t_c}\,d\xi\right] \tag{3}$$

The characteristic thermal time constant is $t_c = \omega_{0e}{}^2/(4D_{th})$. The distribution of the temperature rise represented by eq 3 changes the refractive index accordingly. The wavefront of the probe beam is slightly distorted when it propagates through the illuminated volume of the liquid sample. This distortion can be expressed with an additional phase shift to the probe beam by $\phi(r, t) = (2\pi/\lambda_P)L[n(r, t) - n(0, t)]$,[31,32] where $n(r, t) = n_0 + (dn/dT)T(r, t)$, n_0 is the refractive index, L is the sample thickness, and dn/dT is the temperature coefficient of the refractive index at the probe beam wavelength λ_P. The phase shift can be written in terms of the parameters $m = (\omega_{1P}/\omega_{0e})^2$ and $g = (r/\omega_{1P})^2$ by

$$\phi(g, t) = \frac{\theta}{t_c}\left[\bar{\varepsilon}\int_0^t \frac{1 - e^{-2mg/(1+2\xi/t_c)}}{1 + 2\xi/t_c}\,d\xi + (1 - \bar{\varepsilon})e^{-K_T t}\int_0^t e^{-K_T\xi}\left(\frac{1 - e^{-2mg/(1+2\xi/t_c)}}{1 + 2\xi/t_c}\right)d\xi\right] \tag{4}$$

ω_{1P} is the radius of the probe beam at the sample. The parameter θ measures the strength of the thermal lens effect and is defined by

$$\theta = -\frac{P_e\beta L}{k\lambda_P}\frac{dn}{dT}\varphi \tag{5}$$

After emerging from the sample, the probe beam propagates to the plane of the detector and the intensity of the central portion of the beam is calculated using Fresnel diffraction theory[35] by

$$I(t) = \frac{\left|\int_0^\infty \exp[-(1 + iV)g - i\phi(g, t)]\,dg\right|^2}{\left|\int_0^\infty \exp[-(1 + iV)g]\,dg\right|^2} \tag{6}$$

dx.doi.org/10.1021/jp3119296 | J. Phys. Chem. B 2013, 117, 1932−1937

where $V = Z_1/Z_C$, Z_C is the confocal distance of the probe beam, Z_1 is the distance from the probe beam waist to the sample, and $\phi(g,t)$ is the phase shift of the probe beam given by eq 4. $I(t)$ can be computed numerically and can be used to fit the experimental data. m and V are parameters of the experimental setup that were previously determined, and θ, t_c, $\bar{\varepsilon}$, and K_T are obtained from the fits.

EXPERIMENTAL SECTION

The thermal lens apparatus used in this study is illustrated in Figure 1. Both the excitation and probe lasers are TEM_{00} cw

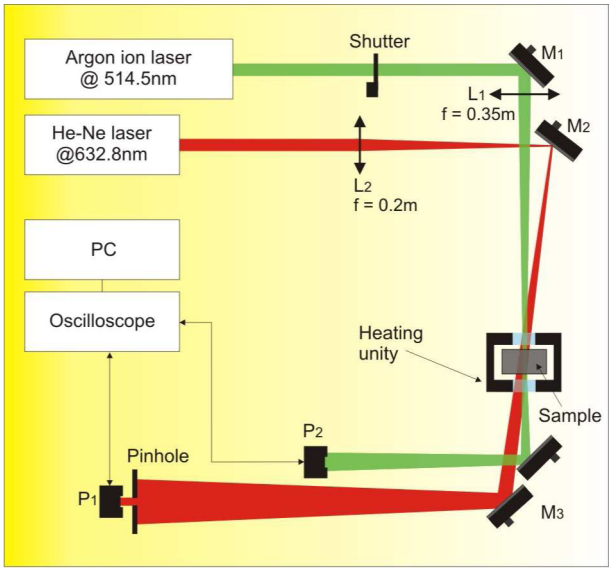

Figure 1. Schematic of the experimental setup used: M_i, mirrors; L_i, lenses; P_i, photodiodes. The experimental parameters are ω_{0e} = 70.0 μm, ω_{1P} = 415.0 μm, Z_1 = 9.8 cm, Z_C = 1.3 cm, m = 35.1, and V = 7.5.

Gaussian beams. An argon ion laser at λ_e = 514.5 nm (Coherent, Model Innova 90) and a He−Ne laser at λ_P = 632.8 nm (Melles Griot, Model 25-LHR-151-249) are used to excite the sample and to probe it, respectively. A mechanical shutter (Thorlabs, Model SH05) controls the exposure of the sample to the excitation laser beam. The excitation beam is focused on the sample using a lens L_1 with a focal length of f = 35 cm. The probe beam is focused by a lens L_2 with f = 20 cm and passes through the sample approximately collinear with the excitation beam. The probe beam propagates to photodiode P_1 (Thorlabs, Model DET100A/M) positioned in the far-field at a distance of >4 m. A pinhole and laser line filter assembly are attached to P_1. The signal from P_1 is recorded by a digital oscilloscope (Tektronix, Model TDS 1001B), which is triggered by photodiode P_2 (Thorlabs, Model PDA10A).

The liquid samples are contained in quartz cuvettes of L = 0.5 cm in a furnace connected to a temperature controller (Lake Shore, Model 340). Thermal lens transient signals are recorded at different excitation laser power levels and at different temperatures.

An optical interferometer experimental system, previously described in ref 36, is used to measure the temperature dependence of the temperature coefficient of the refractive index (dn/dT) of the solutions. In this method, the sample is heated uniformly, and the interference between the reflections of a He−Ne laser beam at 632.8 nm from both cuvette surfaces creates a temperature-dependent interferogram, which can be used to calculate dn/dT.

A stock solution of 68.8 μM eosin Y was prepared by dissolving 2.38 mg of eosin Y in Milli-Q water (Millipore Water Purification System). The stock solution was diluted in 25.0 mL of Milli-Q water to obtain a low concentration of 43.5 nM for the thermal lens measurements. In addition, higher concentrations were also prepared to measure the optical absorption coefficient at different temperatures. A UV/vis spectrophotometer (Perkin-Elmer, Model LAMBDA 1050) was used to measure the absorbance of the higher concentration solutions at 514.5 nm, and the results were used to calculate the optical absorption coefficient of the low concentration solution by extrapolating the data at higher concentrations. The emission spectrum was measured using a fluorescence spectrometer (Perkin-Elmer, Model LS 45) at an excitation wavelength of 514.5 nm. Pure water was also measured using the thermal lens setup. The solutions were prepared immediately before each experiment.

RESULTS AND DISCUSSION

Figure 2a shows the absorption and emission spectra of a 2.2 μM aqueous solution of eosin Y at T = 21 °C. There is an

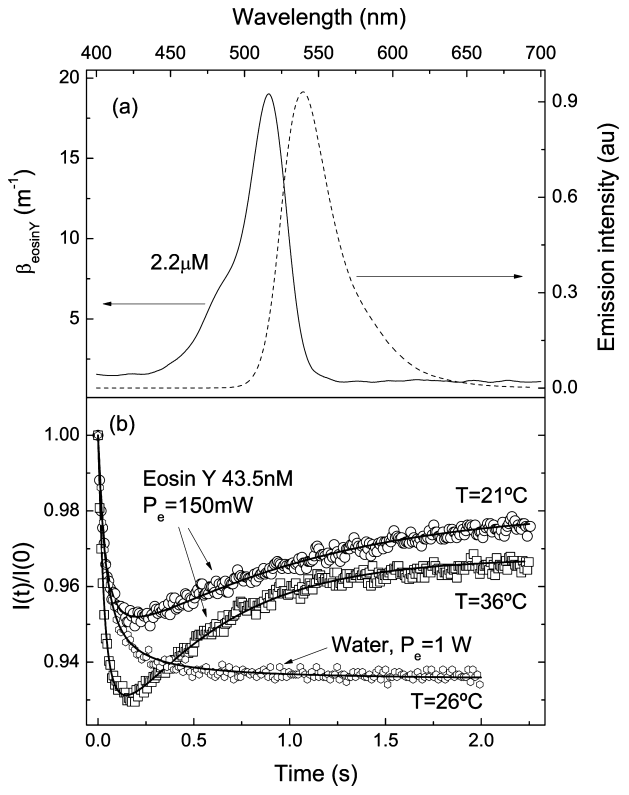

Figure 2. (a) Optical absorption coefficient and emission spectra of an aqueous solution of eosin Y. (b) (open symbols) Normalized thermal lens transient signals and (continuous lines) the best fit curves with $I(t)$.

intense band at 517 nm, corresponding to the monomeric form of eosin Y, with a shoulder at 494 nm, corresponding to the dimeric form of eosin Y, as previously reported.[2] The emission spectrum has a maximum at around 540 nm and a mean emission wavelength of $\langle\lambda_{em}\rangle$ = 547 nm. The optical absorption coefficient of the 43.5 nM aqueous solution at 514.5 nm was

dx.doi.org/10.1021/jp3119296 | J. Phys. Chem. B 2013, 117, 1932−1937

calculated by extrapolating the values obtained at higher concentrations and at different temperatures.

The thermal lens experiments were performed at five different temperatures from 21 to 41 °C on pure water and 43.5 nM aqueous solutions of eosin Y. At each temperature, five different excitation powers, from 150 to 460 mW, were used. At each excitation power, several transients were averaged. Figure 2b presents one transient at 26 °C for pure water and two transients for eosin Y at 21 and 36 °C, in which the effect of photobleaching on the thermal lens signal is clearly observed. On exposing the eosin Y solutions to the excitation laser beam, the intensity of the central portion of the probe beam decreases for a very short time (<100 ms), during which only thermal effects are supposed to occur. Thereafter, photobleaching suppresses the thermal effects by reducing the concentration of absorbing species in the excited volume. The signal eventually reaches a steady state in which photobleaching and mass diffusion alter the concentration of the absorbing species in the excited region to approach a relatively stable value. This process is discussed below.

The photobleaching process observed in this solution is driven by the production of singlet oxygen. The cw laser excites molecules from the ground state to the first excited singlet band following thermalization of the sensitizer to the lowest excited singlet state. Radiative relaxation—spontaneous emission—and internal conversion to the ground state occur from the first excited state band; these processes give rise to the fluorescence observed in Figure 2a as well as nonradiative relaxation—heat generation. In addition, intersystem crossing produces the sensitizer triplet state, thereby allowing this triplet state to generate singlet oxygen through an energy transfer process assisted by collision of the sensitizer with triplet oxygen. The eosin Y molecules produce on the order of 10^4 molecules of singlet oxygen $^1O_2$ before being degraded through photobleaching by $^1O_2$ or through other processes.[18]

The thermal lens technique measures the slow process of the photobleaching of eosin Y molecules by $^1O_2$. This process can be evaluated by fitting the transient signals of the eosin Y solution to the thermal lens model. In this very dilute solution, the thermal and optical properties (D_{th} and dn/dT) are expected to follow those of pure water. For this reason, we performed thermal lens measurements on pure water at the same temperatures, and using eq 4 with $K_T = 0$, the transients were fitted to the model without photobleaching[31,32]—$I(t)$. The temperature dependence of the thermal diffusivity and θ_{water}/P_e of pure water are presented in Figure 3. D_{th} varied from $(1.41 \pm 0.05) \times 10^{-7}$ m^2 s^{-1} at 21 °C to $(1.67 \pm 0.06) \times 10^{-7}$ m^2 s^{-1} at 41 °C. D_{th} was later fixed and used to fit the transients of the eosin Y solution. The continuous lines in Figure 2b represent the fit to $I(t)$ and eq 4. The parameters θ, $\bar{\varepsilon}$, and K_T are obtained from the regressions. At 21 °C, $\theta_{eosinY} = (0.048 \pm 0.005)$, $\bar{\varepsilon} = (0.27 \pm 0.02)$, and $K_T = (1.2 \pm 0.1)$ s^{-1}, and at 36 °C, $\theta_{eosinY} = (0.071 \pm 0.002)$, $\bar{\varepsilon} = (0.33 \pm 0.01)$, and $K_T = (2.0 \pm 0.1)$ s^{-1}. The normalized θ_{eosinY}/P_e as a function of temperature is presented in Figure 3.

The parameter θ/P_e gives information on the physical properties of the solution. For instance, it can be used to calculate the optical absorption coefficient of pure water, using $\varphi = 1$ in eq 5, provided k and dn/dT are known. $k = D_{th}\rho c$ was calculated from the measured D_{th} and the specific heat and mass density of water.[37] At 21 °C, $k = (0.59 \pm 0.03)$ W m^{-1} K^{-1}, which is in agreement with the literature values for water.[37] Figure 4a shows the measured values of dn/dT for water using

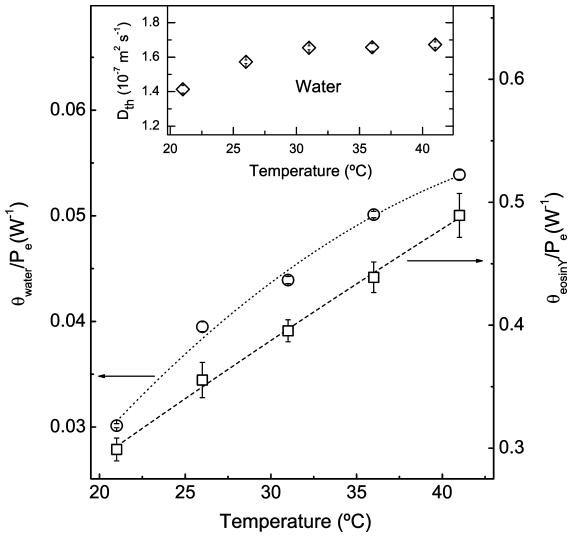

Figure 3. Temperature dependence of θ/P_e obtained from fits of the thermal lens transient signals for pure water (open circles) and eosin Y (open squares). The dashed and dotted lines are guides to the eye.

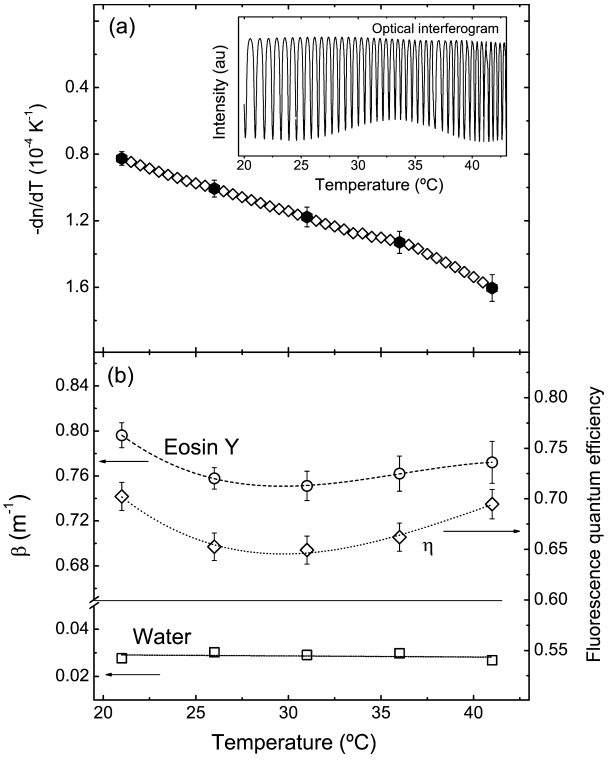

Figure 4. (a) Temperature dependence of dn/dT for pure water. (b) Optical absorption coefficients and fluorescence quantum efficiency for water and eosin Y solutions. The inset in part a shows the temperature dependence of the optical interferogram. The dashed and dotted lines in part b are guides to the eye.

the optical interferometer. The temperature coefficient decreases approximately linearly with temperature, varying from $-(0.82 \pm 0.02) \times 10^{-4}$ K^{-1} at 21 °C to $-(1.60 \pm 0.03) \times 10^{-4}$ K^{-1} at 41 °C. The inset shows the interferogram. By substituting these values for dn/dT into eq 5, the optical absorption coefficient of water can be evaluated. The optical absorption coefficients of water and the eosin Y solution are shown in Figure 4b. For the eosin Y solution, $\varphi = 1 - \eta\lambda_e/$

dx.doi.org/10.1021/jp3119296 | J. Phys. Chem. B 2013, 117, 1932−1937

$\langle\lambda_{em}\rangle$, where λ_e is the excitation beam wavelength, $\langle\lambda_{em}\rangle$ is the mean emission wavelength, and η is the fluorescence quantum efficiency. Using eq 5 for water and eosin Y, one can write

$$\frac{\theta_{eosinY}/P_e}{\theta_{water}/P_e} = \frac{\beta_{eosinY}}{\beta_{water}}\left(1 - \eta\frac{\lambda_e}{\langle\lambda_{em}\rangle}\right) \quad (7)$$

Note that dn/dT, L, λ_p, and k were assumed to be the same for the dilute eosin Y solution and for water. With these parameters, the fluorescence quantum efficiency was calculated and the results are presented in Figure 4b. The high value for η at 21 °C, (0.70 ± 0.02), is within the range of reported values for organic dyes,[26,38,39] 0.4−0.8.

The parameters found for the eosin Y solution from the regression of the data are related to the rate constant and the concentrations of the species in the theoretical model. The rate constant K_T obtained from the fit of the eosin Y signals to the model was found to have a linear dependence on the excitation power P_e as $K_T = K_m + K_{pb}(P_e)$. The same behavior is observed for all the temperatures analyzed. From the linear regression of K_T versus P_e, plots of the linear K_m and angular K_{pb} coefficients of K_T/P_e are shown in Figure 5a. K_m increases from 0.82 ± 0.04

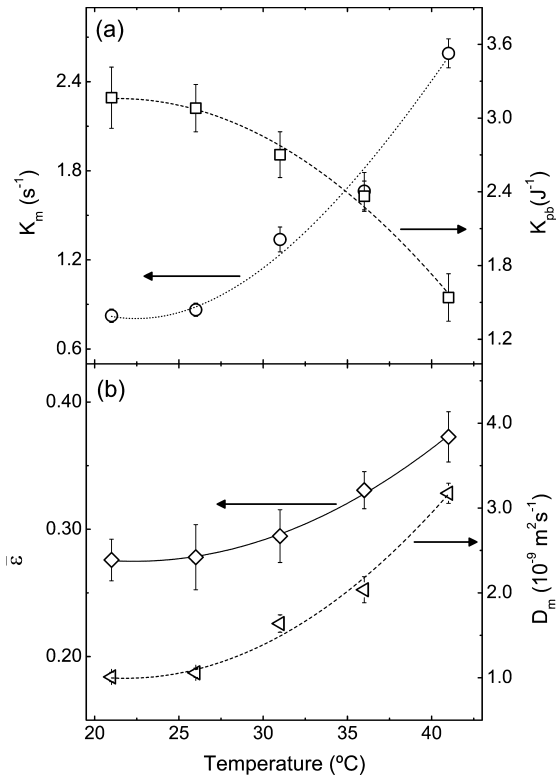

Figure 5. Temperature dependence of (a) K_m and K_{pb} and (b) $\bar{\varepsilon}$ and D_m. The dashed and dotted lines are guides to the eye.

s^{-1} at 21 °C to 2.6 ± 0.1 s^{-1} at 41 °C, whereas K_{pb} decreases from 3.2 ± 0.2 to 1.6 ± 0.1 J^{-1} in the same temperature range. A plot of $\bar{\varepsilon}$ with temperature is also shown in Figure 5b.

Diffusion of the absorbing species should not depend on the excitation power. This, in fact, corresponds to the linear parameter K_m or the molecular diffusion rate constant, which can be thought of as being related to the molecular diffusion time constant through $\tau_m = K_m^{-1}$. Consequently, τ_m relates to the molecular diffusion coefficient, through $D_m = \omega_{0e}^2/(4\tau_m)$. At 21 °C, a value of D_m = (1.00 ± 0.05) × 10^{-9} m^2 s^{-1} was determined, which is within the range of values reported in the literature for fluorescein solutions.[40−43] The temperature dependence of D_m is presented in Figure 5b. This behavior is also observed in other organic dyes in water.[42,43] In turn, K_{pb} is related to the photobleaching degradation process of eosin Y. K_{pb} decreases as temperature increases; this decrease indicates a possible reduction in the absorption cross section as the temperature increases. In contrast, $\bar{\varepsilon}$ shows that the molar absorptivity of the products in the illuminated area increases as temperature increases.

It is important to note that a complete evaluation of the photobleaching of a sensitizer is a complex problem, and identification of the individual contributions to the thermal lens signal is always challenging. Although complex, the problem can be qualitatively and quantitatively investigated using the thermal lens spectroscopy.

CONCLUSIONS

The results show that the photobleaching of eosin Y has a significant effect on the thermal lens signal. Considering the reaction kinetics and molecular diffusion, we have modeled the optical bleaching. Molecular diffusion drives the photochemically modified species to a steady state, and the transient signal changes accordingly. The model provided quantitative values for the molecular diffusion properties, photobleaching reaction rate, and fluorescence quantum efficiency. The temperature dependences of the physical parameters were found to be in agreement with literature data for organic dyes. Although the model was developed specifically for a first-order or pseudo-first-order relaxation process, it should be suitable for describing more complex systems. The results presented here demonstrate that time-resolved thermal lens spectroscopy can be used as a very sensitive analytical tool for quantitative measurement of relaxation processes in aqueous solutions.

AUTHOR INFORMATION

Corresponding Author

*E-mail: herculano@osamember.org (L.S.H.); astrathngc@pq.cnpq.br (N.G.C.A.).

Notes

The authors declare no competing financial interest.

ACKNOWLEDGMENTS

We acknowledge financial support for this work from the Brazilian agencies CAPES, CNPq, and Fundação Araucária.

REFERENCES

(1) Fleming, G. R.; Knight, A. W. E.; Morris, J. M.; Morrison, R. J. S.; Robinson, G. W. Picosecond Fluorescence Studies of Xanthene Dyes. *J. Am. Chem. Soc.* **1977**, *99*, 4306−4311.

(2) Chakraborty, M.; Panda, A. K. Spectral Behaviour of Eosin Y in Different Solvents and Aqueous Surfactant Media. *Spectrochim. Acta, Part A* **2011**, *81*, 458−465.

(3) del Valle, J. C.; Catalán, J.; Amat-Guerri, F. Comparative Photophysical Study of Rose Bengal, Eosin Y and Their Monomethyl and Dimethyl Derivatives. *J. Photochem. Photobiol., A* **1993**, *72*, 49−53.

(4) Meallier, P.; Guittonneau, S.; Emmelin, C.; Konstantinova, T. Photochemistry of Fluorescein and Eosin Derivatives. *Dyes Pigm.* **1999**, *40*, 95−98.

(5) Grossweiner, L. I.; Zwicker, E. F. Primary Processes in The Photochemistry of Eosin. *J. Chem. Phys.* **1959**, *31*, 1141−1142.

(6) Waheed, A. A.; Gupta, P. D. Estimation of Submicrogram Quantities of Protein Using the Dye Eosin Y. *J. Biochem. Biophys. Methods* **2000**, *42*, 125−132.

(7) Waheed, A. A.; Rao, K. S.; Gupta, P. D. Mechanism of Dye Binding in The Protein Assay Using Eosin Dyes. *Anal. Biochem.* **2000**, *287*, 73−79.
(8) Kim, S.-S.; Yum, J.-H.; Sung, Y.-E. Improved Performance of a Dye-Sensitized Solar Cell Using a TiO_2/ZnO/Eosin Y Electrode. *Sol. Energy Mater. Sol. Cells* **2003**, *79*, 495−505.
(9) Tai, W.-P.; Inoue, K. Eosin Y-Sensitized Nanostructured SnO_2/TiO_2 Solar Cells. *Mater. Lett.* **2003**, *57*, 1508−1513.
(10) Mali, S. S.; Betty, C. A.; Bhosale, P. N.; Patil, P. S. Eosin-Y and N_3-Dye Sensitized Solar Cells (DSSCs) Based on Novel Nanocoral TiO_2: A Comparative Study. *Electrochim. Acta* **2012**, *59*, 113−120.
(11) Hazebroucq, S.; Labat, F.; Lincot, D.; Adamo, C. Theoretical Insights on the Electronic Properties of Eosin Y, An Organic Dye for Photovoltaic Applications. *J. Phys. Chem. A* **2008**, *112*, 7264−7270.
(12) Lapidoth, M.; Ben, A. D.; Bhandarkar, S.; Fried, L.; Arbiser, J. L. Efficacy of Topical Application of Eosin for Ulcerated Hemangiomas. *J. Am. Acad. Dermatol.* **2009**, *60*, 350−351.
(13) Wilkinson, F.; Helman, W. P.; Ross, A. B. Quantum Yields for the Photosensitized Formation of the Lowest Electronically Excited Singlet-State of Molecular-Oxygen in Solution. *J. Phys. Chem. Ref. Data* **1993**, *22*, 113−262.
(14) Niedre, M.; Patterson, M. S.; Wilson, C. Direct Near-Infrared Luminescence Detection of Singlet Oxygen Generated by Photodynamic Therapy in Cells in Vitro and Tissues in Vivo. *J. Photochem. Photobiol.* **2002**, *75*, 382−391.
(15) Gerola, A. P.; Semensato, J.; Pellosi, D. S.; Batistela, V. R.; Rabello, B. R.; Hioka, N.; Caetano, W. Chemical Determination of Singlet Oxygen From Photosensitizers Illuminated With LED: New Calculation Methodology Considering the Influence of Photobleaching. *J. Photochem. Photobiol., A* **2012**, *232*, 14−21.
(16) Knox, J. P.; Dodge, A. D. The Photodynamic-Action of Eosin, A Singlet-Oxygen Generator - The Inhibition of Photosynthetic Electron-Transport. *Planta* **1985**, *164*, 30−34.
(17) Amat-Guerri, F.; López-González, M. M. C.; Martínez-Utrilla, R. S. Singlet Oxygen Photogeneration by Ionized and Un-Ionized Derivatives of Rose-Bengal and Eosin Y in Diluted Solutions. *J. Photochem. Photobiol., A* **1990**, *53*, 199−210.
(18) DeRosa, M. C.; Crutchley, R. J. Photosensitized Singlet Oxygen and Its Applications. *Coord. Chem. Rev.* **2002**, *233−234*, 351−371.
(19) Martínez, G.; Bonnett, R. Photobleaching of Sensitisers Used in Photodynamic Therapy. *Tetrahedron* **2001**, *57*, 9513−9547.
(20) Kearns, D. R. Physical and Chemical Properties of Singlet Molecular Oxygen. *Chem. Rev.* **1971**, *71*, 395−427.
(21) Chin, K. K.; Trevithick-Sutton, C. C.; McCallum, J.; Jockusch, S.; Turro, N. J.; Scaiano, J. C.; Foote, C. S.; Garcia-Garibay, M. A. Quantitative Determination of Singlet Oxygen Generated by Excited State Aromatic Amino acids, Proteins, and Immunoglobulins. *J. Am. Chem. Soc.* **2008**, *130*, 6912−6913.
(22) Arakane, K.; Ryu, A.; Takarada, K.; Masunaga, T.; Shinmoto, K.; Kobayashi, R.; Mashiko, S.; Nagano, T.; Hirobe, M. Measurement of 1268 nm Emission for Comparison of Singlet Oxygen $^1\Delta_g$ Production Efficiency of Various Dyes. *Chem. Pharm. Bull.* **1996**, *44*, 1−4.
(23) Brennetot, R.; Georges, J. Transient Absorption of the Probe Beam by the Erythrosine Triplet in Pulsed-Laser Thermal Lens Spectrometry: The Influence of the Solvent, Oxygen and Dye Concentration. *Chem. Phys. Lett.* **1998**, *289*, 19−24.
(24) Fuke, K.; Ueda, M.; Itoh, M. Thermal Lensing Study of Singlet Oxygen Reactions. *J. Am. Chem. Soc.* **1983**, *105*, 1091−1096.
(25) Braslavsky, S. E.; Heibel, G. E. Time-Resolved Photothermal and Photoacoustic Methods Applied to Photoinduced Processes in Solution. *Chem. Rev.* **1992**, *92*, 1381−1410.
(26) Chartier, A.; Georges, J.; Mermet, J. M. Limitation of the Thermal-Lens Method in Fluorescence Quantum-Yield Measurements. *Chem. Phys. Lett.* **1990**, *171*, 347−352.
(27) Chartier, A.; Bialkowski, S. E. Optical Bleaching in Continuous Laser-Excited Photothermal Lens Spectrometry. *Appl. Spectrosc.* **2001**, *55*, 84−91.
(28) Bialkowski, S. E. Steady-State Absorption Rate Models for Use in Relaxation Rate Studies With Continuous Laser Excited Photothermal Lens Spectrometry. *Photochem. Photobiol. Sci.* **2003**, *2*, 779−787.
(29) Terazima, M.; Hirota, N.; Shinohara, H.; Saito, Y. Photothermal Investigation of the Triplet-State of C_6O. *J. Phys. Chem.* **1991**, *95*, 9080−9085.
(30) Pedreira, P. R. B.; Hirsch, L. R.; Pereira, J. R. D.; Medina, A. N.; Bento, A. C.; Baesso, M. L.; Rollemberg, M. C. E.; Franko, M. Observation of Laser Induced Photochemical Reaction of Cr(VI) Species in Water During Thermal Lens Measurements. *Chem. Phys. Lett.* **2004**, *396*, 221−225.
(31) Astrath, N. G. C.; Astrath, F. B. G.; Shen, J.; Zhou, J.; Michaelian, K. H.; Fairbridge, C.; Malacarne, L. C.; Pedreira, P. R. B.; Medina, A. N.; Baesso, M. L. Thermal-Lens Study of Photochemical Reaction Kinetics. *Opt. Lett.* **2009**, *34*, 3460−3462.
(32) Herculano, L. S.; Astrath, N. G. C.; Malacarne, L. C.; Rohling, J. H.; Tanimoto, S. T.; Baesso, M. L. Laser-Induced Chemical Reaction Characterization in Photosensitive Aqueous Solutions. *J. Phys. Chem. B* **2011**, *115*, 9417−9420.
(33) Malacarne, L. C.; Astrath, N. G. C.; Medina, A. N.; Herculano, L. S.; Baesso, M. L.; Pedreira, P. R. B.; Shen, J.; Wen, Q.; Michaelian, K. H.; Fairbridge, C. Soret Effect and Photochemical Reaction in Liquids With Laser-Induced Local Heating. *Opt. Express* **2011**, *19*, 4047−4058.
(34) Astrath, N. G. C.; Astrath, F. B. G.; Shen, J.; Zhou, J.; Michaelian, K. H.; Fairbridge, C.; Malacarne, L. C.; Pedreira, P. R. B.; Santoro, P. A.; Baesso, M. L. Arrhenius Behavior of Hydrocarbon Fuel Photochemical Reaction Rates by Thermal Lens Spectroscopy. *Appl. Phys. Lett.* **2009**, *95*, 191902-1−191902-3.
(35) Shen, J.; Snook, R. D. Thermal Lens Measurement of Absolute Quantum Yields Using Quenched Fluorescent Samples as References. *Chem. Phys. Lett.* **1989**, *155*, 583−586.
(36) Steimacher, A.; Medina, A. N.; Bento, A. C.; Rohling, J. H.; Baesso, M. L.; Reynoso, V. C. S.; Lima, S. M.; Petrovich, M. N.; Hewak, D. W. The Temperature Coefficient of the Optical Path Length as a Function of the Temperature in Different Optical Glasses. *J. Non-Cryst. Solids* **2004**, *348*, 240−244.
(37) Lide, D. R. *CRC Handbook of Chemistry and Physics*, 88th ed.; CRC Press: Cleveland, OH, 1977.
(38) Martin, M. M. Hydrogen-Bond Effects on Radiationless Electronic-Transitions in Xanthene Dyes. *Chem. Phys. Lett.* **1975**, *35*, 105−111.
(39) Olmstead, J., III. Calorimetric Determinations of Absolute Fluorescence Quantum Yields. *J. Phys. Chem.* **1979**, *83*, 2581−2584.
(40) Culbertson, C. T; Jacobson, S. C.; Ramsey, J. M. Diffusion Coefficient Measurements in Microfluidic Devices. *Talanta* **2002**, *56*, 365−373.
(41) Gendron, P.-O.; Avaltroni, F.; Wilkinson, K. J. Diffusion Coefficients of Several Rhodamine Derivatives as Determined by Pulsed Field Gradient-Nuclear Magnetic Resonance and Fluorescence Correlation Spectroscopy. *J. Fluoresc.* **2008**, *18*, 1093−1101.
(42) Delgado, J. M. P. Q. Molecular Diffusion Coefficients of Organic Compounds in Water at Different Temperatures. *J. Phase Equilib. Diffus.* **2007**, *28*, 427−432.
(43) Holz, M.; Heil, S. R.; Sacco, A. Temperature-Dependent Self-Diffusion Coefficients of Water and Six Selected Molecular Liquids for Calibration in Accurate ^1H NMR PFG Measurements. *Phys. Chem. Chem. Phys.* **2000**, *2*, 4740−4742.